Giant resonances in ^{40}Ca

Y.-W. Lui, J. D. Bronson, C. M. Rozsa,* D. H. Youngblood, P. Bogucki, and U. Garg
Cyclotron Institute, Texas A&M University, College Station, Texas 77843
(Received 18 May 1981)

Inelastic scattering of 98.5, 116.8, and 129.4 MeV α particles from ^{40}Ca has been measured. Analyses were performed on the region between 13.2 to 22.5 MeV excitation energy. From the angular distributions, states at 13.9 and 14.6 MeV have been identified as 0^+ and 2^+, and exhaust 6 and 2.5% of the corresponding energy-weighted sum rule, respectively. Structure at about 15.8 MeV can be tentatively assigned 3^-. The giant quadrupole resonance at $E_x = 17.7 \pm 0.2$ MeV exhausting 48 ± 8 % of $E2$ energy-weighted sum rule dominates the spectra in this energy region. The giant monopole resonance is not observed. The angular distribution of the 10.6 MeV state shows 1^- characteristics and can be explained as an isoscalar dipole state.

[NUCLEAR REACTIONS ^{40}Ca(α,α'), $E_\alpha = 98.5$, 116.8, and 129.4 MeV: measured E_x, $\sigma(\theta)$ giant resonances, deduced L,β.]

I. INTRODUCTION

The systematic characteristics of the giant quadrupole resonance (GQR) have been well established from ^{13}N to ^{232}Th (Ref. 1.). Over this entire range, the excitation energy of the GQR follows approximately $E_x = 63A^{-1/3}$, although in lighter nuclei, it is somewhat below this value. Recently, there has been considerable interest in the giant monopole resonance (GMR) since its energy can be directly related to the nuclear incompressibility. In experiments utilizing inelastically scattered hadrons,[2-5] the GMR has been located slightly above the GQR and tends to follow $E_x \approx 76A^{-1/3}$ in medium and heavier nuclei ($A \geq 64$).

Many experiments have been performed in the search for GMR strength in lighter nuclei and there are several reports on isoscalar multipole resonances in ^{40}Ca. However, the results are not conclusive. In general, a broad peak at around 18 MeV excitation energy has been identified as the GQR, and its parameters have been determined by measurements of inelastic scattering of electrons[6] and hadrons.[3,7,8] Nevertheless, there are ambiguities about multipole strength distributions and spin assignments around the GQR region.

In their early inelastic deuteron experiments, Marty *et al.*[9] reported that the GMR in ^{40}Ca was located at $E_x \approx 20$ MeV. This group[10] has recently suggested that monopole strength underlies the energy range between 14 to 23 MeV, with a small concentration at 14 MeV; however, there are inherent uncertainties in the continuum analysis as well as ambiguities in extracting monopole strength from deuteron experiments. Bertrand *et al.*[3] studied the giant resonance region in ^{40}Ca with inelastically scattered protons and concluded that they saw no evidence for the GMR. Inelastic ^{3}He scattering[11] also suggested that monopole strength was present in the energy range from 12 to 20 MeV but recorded no evidence for $E0$ strength above 20 MeV. In a correlation experiment between inelastically scattered ^{3}He particles and decay α particles from the giant resonance region of ^{40}Ca performed by Yamagata *et al.*[12] a new 0^+ state at 14.2 MeV, the GQR at 18 MeV, and possible octupole strength at around 16.7 MeV were reported; however, no other monopole strength was reported. More recently, inelastic scattering experiments with 104 MeV α particles have been done,[13] where the GQR at about 18 MeV, some $E1$ strength (suggested to be isoscalar) between 13.3 and 16.7 MeV, and $E0$ strength between 20.3 and 21.7 MeV were reported. Inelastic pion scattering[14] from ^{40}Ca at 163 and 244 MeV incident energies has also been studied. The GQR located at about 18 MeV was strongly excited and

some evidence for a GMR was reported, but the results at different bombarding energies were inconsistent.

In this paper, we present recent analyses of ^{40}Ca data which have been obtained in this laboratory during the past few years. These analyses yield additional information which resolves some of the disagreements about strength distributions and multipolarity assignments in the giant resonance region.

II. EXPERIMENTAL SETUP AND PROCEDURE

Beams of 98.5, 116.8, and 129.4 MeV α particles were provided by the Texas A&M University variable energy cyclotron. The beam energies were analyzed by a 160° magnet to 50 keV energy spread and then passed through three sets of horizontal and vertical slits placed along the beam line to clean up beam halo before impinging on a natural Ca target. The targets were prepared in vacuum evaporation and transferred to the scattering chamber in a dry nitrogen atmosphere to reduce oxidation. Target thickness was measured with an alpha source. Inelastically scattered α particles were detected with an 86-cm-long resistive wire proportional counter backed by an NE 102 scintillator placed in the focal plane of the Enge split-pole magnetic spectrograph. Considerable care was taken to minimize background contributions from various secondary scatterings, and an energy resolution of $\simeq 300$ keV, primarily due to straggling in the target, was obtained. A lithium drifted silicon detector telescope placed at 25° was used to monitor the beam integration. Differential cross sections were obtained from the known target thickness, solid angle, and beam charge, including the appropriate dead-time corrections. Details of the experimental setup and procedures are discussed in Ref. 4.

Spectra were taken at laboratory angles from $\theta_{lab} = 3° - 15°$ and $\theta_{lab} = 2° - 9°$ for α-particle energies of 98.5 and 116.8 MeV, respectively. At 129.4 MeV α energy, measurements were made only for $\theta_{lab} = 0°$ and 4°. Experimental data measured from $\theta_{lab} = 13.5° - 35.0°$ at 96 MeV and reported previously[8] have also been reanalyzed.

III. DATA ANALYSES AND RESULTS

Energy spectra for 99, 117, and 129 MeV are shown in Figs. 1, 2, and 3, respectively. The angular distributions of the differential cross section of the 3.74 MeV 3^- state and the corresponding

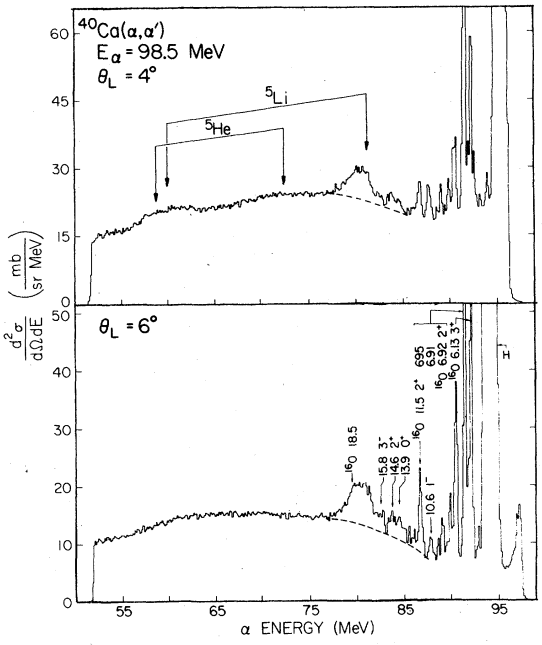

FIG. 1. Spectra of inelastic scattering of 98.5 MeV α particles from ^{40}Ca taken at 4° and 6°. The elastic peak and a few MeV of low excitation were blocked by a Ta sheet. The dashed line indicates the nuclear continuum assumed. Kinematic limits for α particles from ^{5}Li and ^{5}He breakup are also shown. Some of the states in ^{40}Ca and contaminant peaks from ^{16}O are indicated.

distorted-wave Born approximation (DWBA) calculations for 99 and 117 MeV data are shown in Fig. 4. The cross sections were normalized to correspond to the $\beta^2 R^2$ for the 3.74 MeV 3^- state reported in Ref. 8 in order to obtain absolute differential cross sections. DWBA calculations for monopole, dipole, and higher multipole transitions were performed with a modified DWUCK-4 computer code.[15] A standard collective form factor including Coulomb excitation was used for $L \geq 2$ (Ref. 4). For monopole calculations, Satchler's version I form factor[16] was used. The isoscalar dipole calculation was performed using the form factor described in Ref. 17. The optical potentials used in the calculations are the same as those in Ref. 8.

Since the shape of the nuclear continuum underlying the region of interest is not theoretically established, an empirical subtraction technique must be used, which results in large uncertainties in the differential cross sections. The shape assumed for the nuclear continuum was obtained by fitting a linear, quadratic, or higher order curve through the regions of the spectrum below and above the giant resonances (GR) region. The dashed lines in Figs. 1 – 3

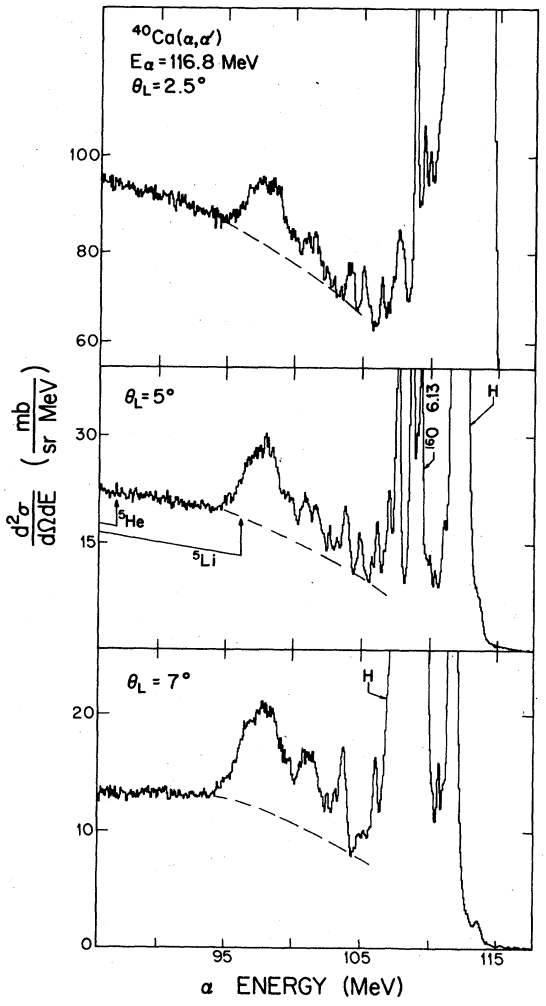

FIG. 2. See Fig. 1 for 116.8 MeV α particles at 2.5°, 5°, and 7°.

indicate the continuum shape chosen. The angular distributions of the double differential cross section of the nuclear continuum underneath the GR region for 99 and 117 MeV data are shown in Fig. 5. They show a smooth dependence on angle. The rise at extreme forward angles is likely due to an introduction of real background from slit scattering. The GR spectra with the nuclear continuum subtracted are shown in Figs. 6—8. It is obvious from the spectra shown in Figs. 6—8 that there are structures in this energy range.

Several different analyses were tried to ascertain the character of the strength observed. After subtraction of the nuclear continuum, the 99 MeV data was analyzed by integrating the three regions between 15.2 and 21.7 MeV which are labeled in Fig. 6. The angular distributions of the differential

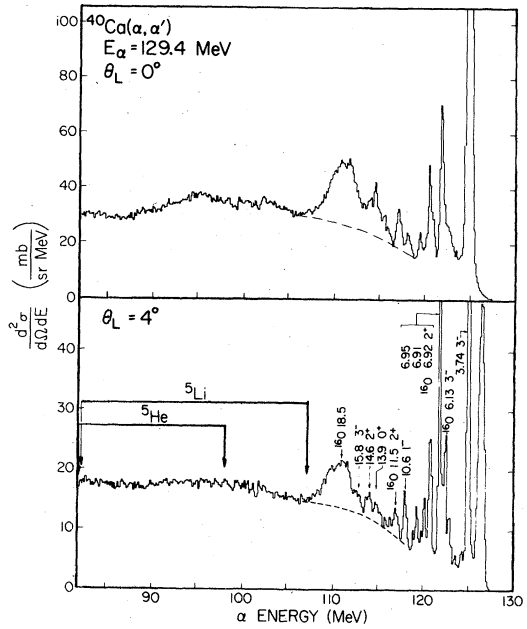

FIG. 3. See Fig. 1 for 129.4 MeV α particles at 0° and 4°.

cross sections for different regions are shown in Fig. 9. A slightly different regional analysis was carried out for both the 99 MeV data (together with the 96 MeV data) covered from $\theta_{lab} = 3°-35°$ and the 117 MeV data by integrating each of four regions between 13.2 and 22.5 MeV as labeled in Fig. 7. The angular distributions of the differential cross section of each of these regions are shown together with DWBA calculations in Figs. 10 and 11. In order to extract more detailed information, analyses concentrating on peaks or structures between 10.0 and 16.3 MeV were performed. The energy resolution is not sufficient to resolve all the true structures; however, four peaks or peaklike structures were analyzed. The angular distributions of the differential cross sections of each peak or structure are

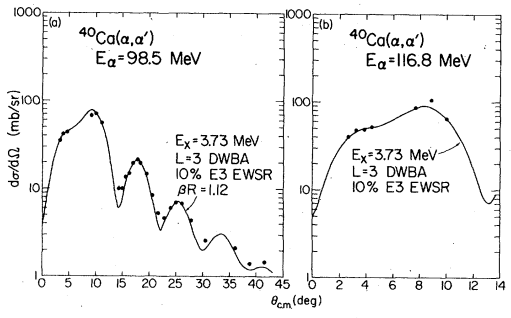

FIG. 4. Angular distributions of the 3.74 MeV 3^- state obtained for (a) 98.5 and (b) 116.8 MeV α energies.

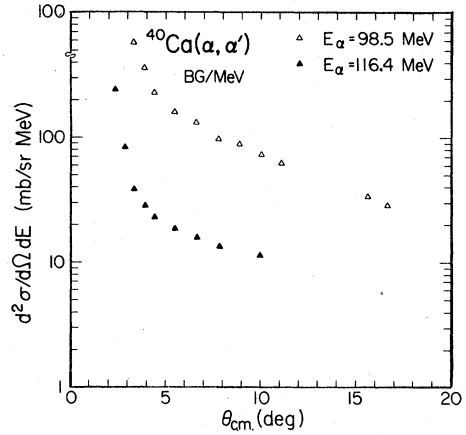

FIG. 5. Angular distributions of the nuclear continuum under the giant resonance region.

shown in Figs. 12 and 13 with DWBA calculations superimposed on the data. The error bars in the differential cross sections represent not only the statistical uncertainty but also the uncertainties in nuclear continuum subtraction. These are much

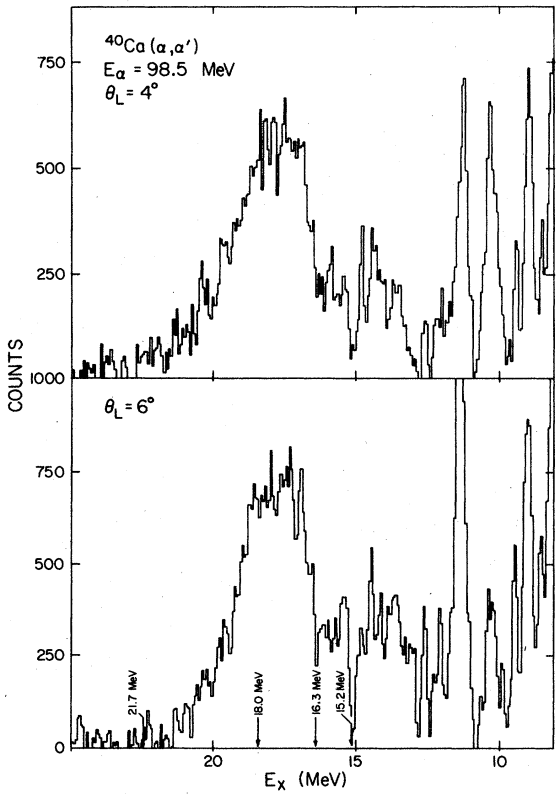

FIG. 6. Portions of spectra of inelastically scattered 98.5 MeV α particles from ^{40}Ca taken at 4° and 6° after subtraction of the continuum.

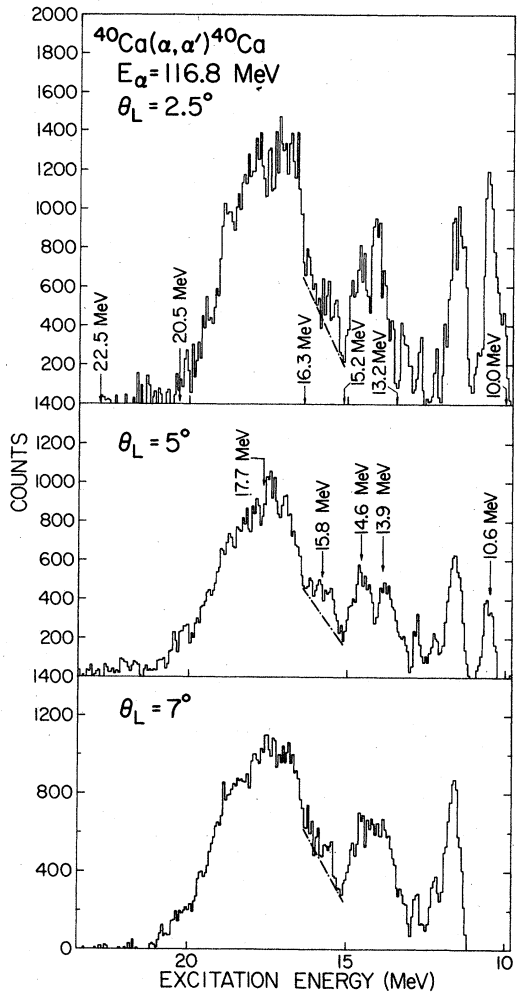

FIG. 7. Same as Fig. 6 for 116.4 MeV α particles at 2.5°, 5°, and 7°. The dot-dashed line indicates the assumed background for the possible 3^- resonance.

bigger than the statistical uncertainty. The contrast between the smooth angular distribution of the nuclear continuum and the diffractive structure of the resonances is an indication that the subtraction of the nuclear continuum has been accomplished in a consistent manner. The L assignments, excitation energies widths, etc., extracted from the present analysis together with the previously published results on ^{40}Ca are listed in Table I. For our results, the excitation energy is the centroid, and the width is the rms width $\times$ 2.35 of the integrated counts in the specified region. An analysis utilizing Gaussian peak fitting of the GR peak region between 16.3 and 21 MeV was also done. Because of the apparent differences in the width of the giant

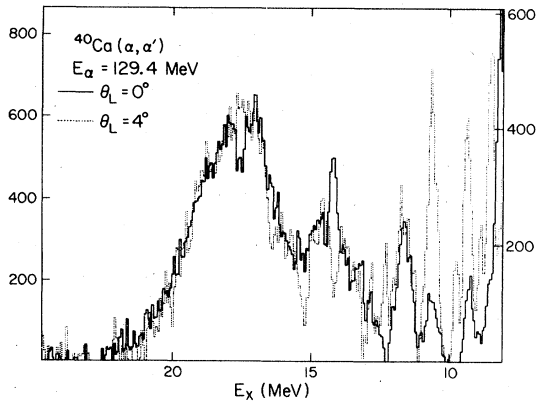

FIG. 8. Portions of continuum-subtracted spectra of inelastically scattered 129.4 MeV α particles from ^{40}Ca taken at 0° and 4° are shown superimposed.

quadrupole resonance peak at different angles and the uncertainties in the overrriding structure in the GR region, reasonable fits could not be obtained for all spectra, especially on the lower excitation region of the GQR peak.

The results of each region are discussed separately below.

A. $E_x = 13.2-15.2$ MeV

The angular distributions of the differential cross section of this region taken at 99 and 117 MeV are reasonably described by $L = 2$ DWBA calculations

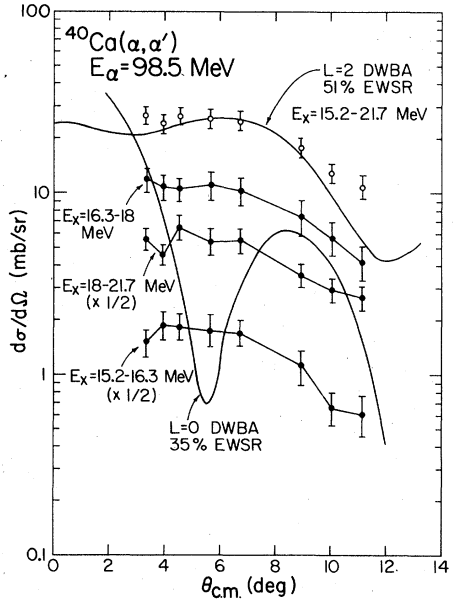

FIG. 9. Angular distributions obtained for portions of the GR peak as labeled in Fig. 6. The distribution for the entire (15.2—22.5 MeV) peak is also shown. DWBA predictions for $L = 0$ and $L = 2$ are shown.

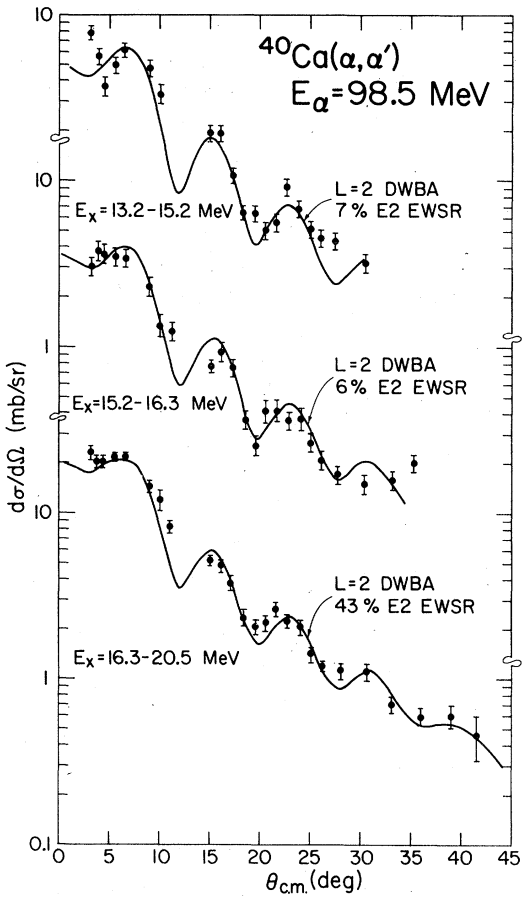

FIG. 10. Angular distributions of the differential cross section of different regions labeled in Fig. 7 for the 98.5 MeV data.

except at angles smaller than 4°. Since it is possible to separate this region into two components at some angles, peak analysis was employed to extract more information. Angular distributions and DWBA predictions for these two components are shown in Figs. 12 and 13 for 99 and 117 MeV, respectively. The 13.9 MeV component is best characterized by $L = 0$ while the 14.6 MeV component is dominated by $L = 2$. The 13.9 MeV component exhausts 6 and 7% of $E0$ energy weighted sum rule (EWSR) for the 99 and 117 MeV data, while the 14.6 MeV component exhausts 4 and 2.5% of $E2$ EWSR for 99 and 117 MeV data, respectively. The uncertainty on the EWSR is estimated to be about $\pm$ 25%. In an experiment measuring particle decay from the giant resonance region of ^{40}Ca (Ref. 18) excited with 115 MeV alpha particles, a peak in α_0 decay events was observed at about 14 MeV. The angular correlation for this group was charateristic of decay of $J^\pi = 2^+$ state and the yield of decay α particles

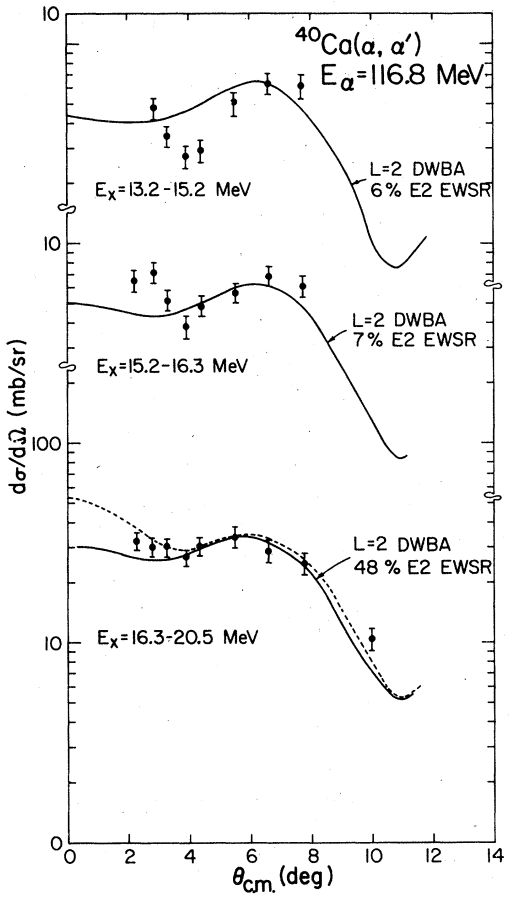

FIG. 11. Same as Fig. 10 for the 116.8 MeV data. The dashed line is the sum of DWBA calculations of $L = 0$ and $L = 2$ (see text).

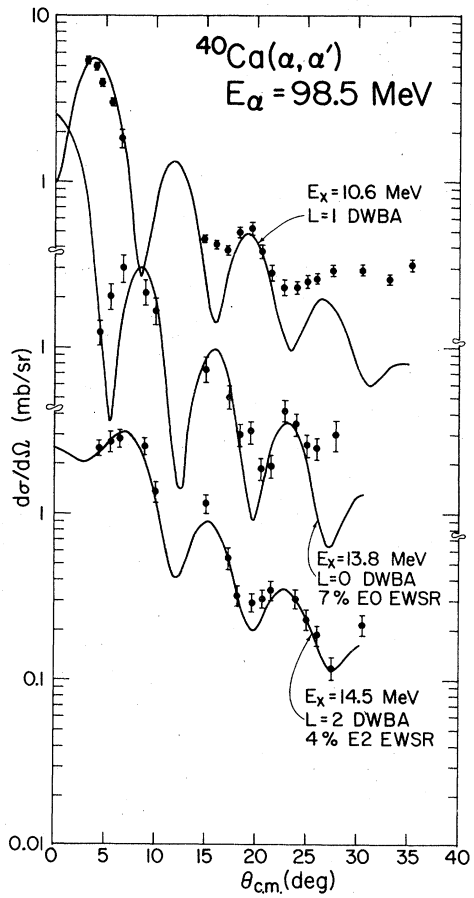

FIG. 12. Angular distributions of the differential cross section of peak analysis between 10.0 and 16.3 MeV for the 98.5 MeV data.

corresponded to about 6 ± 2 % of the $E2$ EWSR. The analysis reported here of the 99 MeV data is consistent with the decay work. The small result obtained at 117 MeV is an indication of the difficulties of untangling the many components in this region. Confirmation of the 0^+ assignment for the 13.9 MeV component has been obtained from the 0° measurement at 129 MeV; as can be seen in Fig. 8 which shows the comparison between the 0° and 4° spectra. The ratio of the cross section for the 13.9 MeV component to that for the 14.6 MeV component at 0° is about 50% larger than that at 4°, as expected. There are clearly other states in this region; however, no definitive spin assignments could be made for those.

B. $E_x = 15.2-16.3$ MeV

The angular distributions of differential cross sections of this region are consistent with an $L = 2$ assignment (see Figs. 10 and 11). The strength above the continuum corresponds to 6 and 7% of $E2$ EWSR for 99 and 117 MeV data, respectively. From the different shape of this region at different angles, it is apparent that there are structures of other multipolarity in this region. Peak analysis was performed by integrating the structure above the dot-dashed line shown in Fig. 7. The angular distribution of differential cross sections of this component is shown in Fig. 13 and can be fitted by an $L = 3$ DWBA calculation assuming that only 0.9% of the $E3$ EWSR is exhausted. The analysis of the same component in the 99 MeV data shows fluctuations in the angular distribution of the differential cross section, and there is no definite sign of an $L = 3$ transfer. It is worth noting that this analysis introduces rather large uncertainties, since the component above the dot-dashed line is superimposed on a dominant $L = 2$ transfer and it is not clear where the background should be drawn.

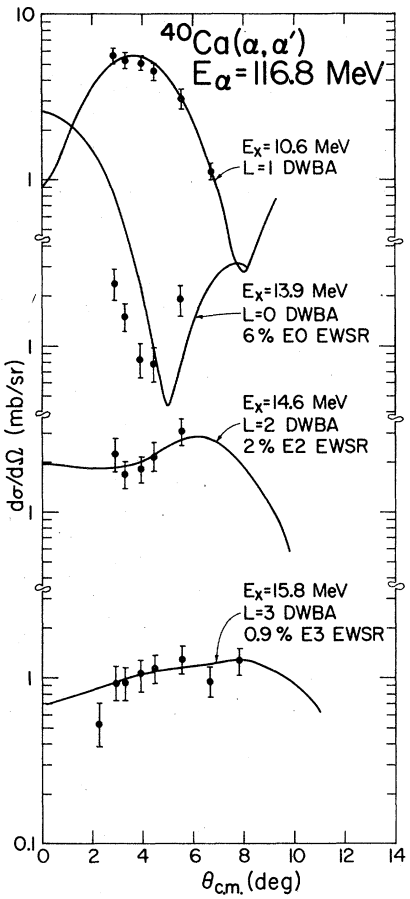

FIG. 13. Same as Fig. 12 for the 116.8 MeV data.

C. $E_x = 16.3-20.5$ MeV

The angular distributions of differential cross sections of this region obtained for the 99 and 117 MeV data are shown in Figs. 10 and 11. The experimental data were fit well by an $L = 2$ DWBA calculation exhausting $43 \pm 9\%$ and $48 \pm 8\%$ $E2$ EWSR for 99 and 117 MeV, respectively. At 129 MeV the strength estimated from the two angles taken (0° and 4°) was 43% $E2$ EWSR. An analysis for different regions of integration (from 16.3 to 18.0 MeV and 18.0 MeV to 21.7 MeV) was performed for the 99 MeV data from $\theta_{lab} = 3°-10°$. The angular distributions obtained for each portion of the giant resonance peak are shown in Fig. 9. It is clear that each portion can be described by an $L = 2$ transfer, and the entire GR peak is also fit well by an $L = 2$ calculation. No evidence of concentrated monopole strength was observed in this region. However, at 129 MeV the differential cross section of the entire GR peak at 0° is about 60% larger than that at 4°, suggesting that significant $E0$ strength may be spread throughout this region. The shape of the GR peak is very similar in the 0° and 4° spectra, which suggests that such monopole strength would have a distribution similar to that of the $E2$ strength. By fitting one Gaussian to the GQR peak in the spectra, an excitation energy of 17.8 ± 0.2 MeV and a width of 3.4 ± 0.5 MeV were obtained. However, because of the apparent difference in the width of the GQR peak at different angles and the uncertainties in the overriding structure in the GR region, a reasonable fit could not be obtained for all spectra.

It is obvious that there are fine structures superimposed on the gross structure of the GQR. These structures could arise from various effects, such as scattering from contaminants in the target, statistical fluctuations, counter effects, or true structures of the multipole resonances. Oxygen contaminant peaks, such as those from states at $E_x = 6.13$ and 11.5 MeV,[19,20] can be seen in the 99 MeV data. The $E_x = 18.5$ MeV state in ^{16}O can barely be seen on the shoulder on the higher excitation side of the GQR. The relative weakness of the $E_x = 6.13$ and 11.5 MeV ^{16}O states compared to the ^{40}Ca states in the 117 and 130 MeV data suggests that the apparent structure in this data does not arise from target contamination. Carbon deposition on the wire of the proportional counter causes a dip and an adjacent peak in the spectrum which occurs at the same channel at all angles and is thus easily identifiable. This can be removed by cleaning or changing the wire. The observed structure is not counter related. The differences in the width of the GQR peak at different angles suggest that there may be other multipole resonances superimposed on the GQR; however, the good agreement between the data and an $L = 2$ calculation (shown in Fig. 10) indicates that other multipole resonances contribute only a small amount of strength in this region.

D. $E_x = 20.5-22.5$ MeV

The spectra in Figs. 1–3 and 6–8 show no apparent structure above the GQR region and the angular distribution of the integrated cross sections shows only random fluctuations. In fact, very little yield remains after the subtraction of the nuclear continuum. At 99 MeV, the (α,Li^5) reaction kinematically overlaps the GQR region, although the contributions from both ^5He and ^5Li breakup are relatively small at this region.[21] It can be seen in Fig. 8 that the energy spectra of 129 MeV data are very similar at 0° and 4°. This contrasts with the experimental data for heavier targets,[4,8] where

TABLE I. Parameters of giant resonances in ^{40}Ca.

Reaction	E_x (MeV)	Γ (MeV)	J^π	% EWSR	Source
(p,p')	18.0 ± 0.3		2^+	49 ± 10	Ref. 7
(p,p')	17.8 ± 0.3	2.5 ± 0.5	2^+	40 ± 10	Ref. 3
$(^3He,^3He')$	18.2	3.0	2^+		Ref. 11
$(^3He,^3He'\alpha)$	14.2	0.2 ± 0.15	0^+	6 ± 3	Ref. 12
	16.7	0.9 ± 0.2	(3^-)	6 ± 3	
	18.2	2.2 ± 0.2	2^+	27 ± 6	
(α,α')	18.1 ± 0.3	3.5 ± 0.3	2^+	44 ± 10	Ref. 8
	17.9 ± 0.3	3.4 ± 0.3	2^+	41 ± 11	
(α,α')	$13.3-15.3$		$1^- + 2^+$	$(4 \pm 1)E2$	Ref. 13
	$15.3-16.7$		$1^- + 2^+$	$(3 \pm 1)E2$	
	$16.7-20.3$		2^+	25 ± 7	
	$20.3-21.7$		0^+	6 ± 3	
(α,α')	10.6 ± 0.2	0.48 ± 0.05	1^-		Present work[a]
	10.6 ± 0.2	0.52 ± 0.08	1^-		Present work[b]
	13.8 ± 0.3	0.40 ± 0.08	0^+	≈ 7	Present work[a]
	13.9 ± 0.3	0.36 ± 0.06	0^+	≈ 6	Present work[b]
	14.5 ± 0.3	0.68 ± 0.08	2^+	≈ 4	Present work[a]
	14.6 ± 0.3	0.51 ± 0.07	2^+	≈ 2.5	Present work[b]
	15.8 ± 0.4	0.63 ± 0.1	3^-	≈ 0.9	Present work
	17.8 ± 0.3	2.25 ± 0.2	2^+	43 ± 9	Present work[a]
	17.7 ± 0.2	2.53 ± 0.4	2^+	48 ± 8	Present work[b]
	18.0 ± 0.3	2.56 ± 0.4	2^+	≈ 43	Present work[c]
(π,π')	18.2	$3.0 - 3.5$	2^+	77	Ref. 14

[a]This value is obtained from the 99 MeV data.
[b]This value is obtained from the 117 MeV data.
[c]This value is obtained from the 130 MeV data.

the GMR appears with a strength comparable to the GQR on the higher excitation side of the GQR at 0°.

E. $E_x = 10.0-13.2$ MeV

There are clearly several components in this region; however, due to the presence of the contamination peak from the 11.5 MeV 2^+ state in ^{16}O between $E_x \approx 11$ and 12 MeV, only the component at $E_x \approx 10.6$ MeV has been analyzed. The angular distributions of the differential cross section of the 10.6 MeV component are shown in Figs. 12 and 13, and they are fit adequately by a calculation using a form factor for an isoscalar dipole state.[17] The underestimation of the cross section by the calculation at the larger angles may suggest the presence of other multipolarities in this region which are not resolved. However, other form factors from the literature[13] give very different predicted cross sections, resulting in EWSR fractions up to an order of magnitude larger. Thus, further investigation of the isoscalar dipole form factor is necessary.

IV. DISCUSSION AND CONCLUSIONS

The present analyses lead to several conclusions that clarify the spin assignments of the resonances around the GR region in ^{40}Ca. The results of the analyses of 99 and 117 MeV data are in excellent agreement. The 10.6 MeV component has been identified as a 1^- state. The small angle measurements ($\theta_{lab} \leq 8°$), especially at 0°, confirm the 0^+ state at $E_x = 13.9$ MeV, while the 14.6 MeV component has been identified as 2^+. This is in reasonable agreement with the results of Yamagata *et al.*[12] who reported a 0^+ state at $E_x = 14.2$ MeV. The 7% of $E2$ EWSR extracted from the larger angle analysis ($\theta_{lab} \geq 13.5°$) in the energy range between 13.2 and 15.3 MeV (see Fig. 10) is in excellent

agreement with our earlier inelastic α-particle data.[8] The $4.0 \pm 1.3\%$ of the $E2$ EWSR exhausted by the 14.6 MeV component for 99 MeV data agrees with the particle decay experiment,[19] while the $2.5 \pm 0.5\%$ of the $E2$ EWSR observed for the same component in the 117 MeV data is lower than that observed in the decay experiment.[18]

The spin and parity of the 15.8 MeV component is most likely 3^-; however, due to the domination of $L = 2$ in that region, this assignment is less definite. The 3^- resonance at 16.7 MeV reported by Yamagata *et al.*[12] has not been observed in this work. From the angular distribution of the differential cross section obtained for the 99 MeV data between $E_x = 16.3$ and 20.5 MeV (see Fig. 10), it is unlikely that a 3^- resonance is located at $E_x = 16.7$ MeV with relatively the same $E2$ and $E3$ strength as seen in the ^{3}He data. Furthermore, the different shape of the spectrum and the relatively different contributions from $E2$ and $E3$ EWSR between ^{3}He (Ref. 12) and α (the present work) suggest that excitation of states in this region by ^{3}He and α particles may be different and not entirely related as predicted in DWBA.

Rost *et al.*[13] reported some $E1$ strength between $E_x = 13.3$ and 16.7 MeV in their measurements of inelastic scattering of 104 MeV α particles; no $E1$ strength has been found in this region in the present analysis. The GQR dominates around 18 MeV and exhausts $40-50\%$ of $E2$ EWSR. This is in excellent agreement with the earlier inelastic α-particle data. The $E2$ EWSR exhausted in this region also agrees with the inelastic proton data.[3,7] However, it is about 20% less than that obtained through inelastic pion scattering[14] and 20% more than that obtained by Yamagata *et al.*[12] Taking into account all of the $E2$ strength between 13.2 and 20.5 MeV, a total of about 56% and 61% of $E2$ EWSR has been observed in the 99 and 117 MeV data, respectively. The excitation energy of the GQR obtained in the present work is in good agreement with that obtained from inelastically scattered protons[3,7] deuterons,[10] ^{3}He's (Ref. 11), and α particles. We see no definitive evidence of $E0$ strength in this region ($E_x = 16.3-20.5$ MeV). The 60% increase in the cross section of the entire GR peak at 0° over 4° (129 MeV data) is consistent with the existence of about 10% of the $E0$ EWSR strength with a centroid and width roughly the same as the GQR (see Fig. 11). This is in agreement with a recent report[11] on monopole resonance strength in light nuclei. If present, this $E0$ strength would not cause a significant deviation from the predominant $E2$ shape of the angular distribution for angles greater than 2°, where the remainder of our data was taken. Further experiments will be required to determine if this $0°-4°$ cross-section difference is in fact due to the presence of 0^+ strength or has other explanations.

Above the GQR region ($E_x > 20.5$ MeV), no evidence of resonancelike structure or $E0$ strength has been observed. This is in disagreement with the results of Rost *et al.*[13] who have reported a small $E0$ strength above the GQR. It should be noted that the poor statistics of their spectrum would introduce large uncertainties in the background subtraction. Furthermore, other reasonable backgrounds can be constructed for the data of Ref. 13, which removes excess yield in the spectrum[13] completely. In any case, identification of weak, broadly distributed strength on top of an ill-defined continuum is at best uncertain and probably requires a definitive demonstration that the angular distribution is significantly different from the continuum.

The fine structure around the GR peak could result from the presence of other weak relatively narrow resonances. This is similar to ^{208}Pb (Ref. 4), where a fit to the GR peak requires two broad Gaussian components (GQR and GMR) and several narrow Gaussian components. This similarity between ^{40}Ca and ^{208}Pb is not unexpected since both of them are closed-shell nuclei and should, therefore, have a smaller level density in the GR region. The good agreement between the experimental data and the corresponding $L = 2$ DWBA calculations shows apparent domination of $L = 2$ in the GR peak. Hence, only a small amount of strength could be assigned to other multipolarities.

This work was supported in part by the National Science Foundation, the Department of Energy, and the Robert A. Welch Foundation.

*Present address: Harshaw Chemical Company, Solon, Ohio 44139

[1]F. E. Bertrand, Annu. Rev. Nucl. Sci. 26, 457 (1976).

[2]D. H. Youngblood, in *Giant Multipole Resonances*, edited by F. E. Bertrand (Harwood, New York, 1980) p. 113; D. H. Youngblood, P. Bogucki, J. D. Bronson, U. Garg, Y.-W. Lui, and C. M. Rozsa, Phys. Rev. C 23, 1997 (1981).

[3]F. E. Bertrand, G. R. Satchler, D. J. Horen, and A. van der Woude, Phys. Lett. 80B, 198 (1979).

[4]D. H. Youngblood, C. M. Rozsa, J. M. Moss, D. R. Brown, and J. D. Bronson, Phys. Rev. Lett 39, 1188 (1977); C. M. Rozsa, D. H. Youngblood, J. D. Bronson, Y.-W. Lui, and U. Garg, Phys. Rev. C 21, 1252 (1980).

[5]Y.-W. Lui, P. Bogucki, J. D. Bronson, U. Garg, C. M. Rozsa, and D. H. Youngblood, Phys. Lett. 93B, 31 (1980).

[6]Y. Torizuka, K. Itoh, Y. M. Shin, Y. Kawazoe, H. Matsuzaki, and G. Takada, Phys. Rev. C 11, 1174 (1975).

[7]N. Marty, M. Morlet, A. Willis, V. Comparat, and R. Frascaria, Nucl. Phys. A238, 93 (1975).

[8]D. H. Youngblood, J. M. Moss, C. M. Rozsa, J. C. Bronson, A. D. Bacher, and D. R. Brown, Phys. Rev. C 13, 994 (1976).

[9]N. Marty, M. Morlet, A. Willis, V. Comparat, R. Frascaria, and J. Kallne, Orsay Report No. IPNO-PH N75-11, 1975.

[10]A. Willis, M. Morlet, N. Marty, R. Frascaria, C. Djalali, V. Comparat, and P. Kitching, Nucl. Phys. A344, 137 (1980).

[11]D. Lebrun, M. Buenerd, P. Martin, P. de Saintignon, and G. Perrin, Phys. Lett. 97B, 358 (1980).

[12]T. Yamagata, K. Iwamoto, S. Kishimoto, B. Sacki, K. Yhasa, M. Tanaka, T. Fukuda, K. Okada, I. Miura, M. Inour, and H. Ogata, Phys. Rev. Lett. 40, 1628 (1978).

[13]H. Rost, W. Eyrich, A. Hofmann, U. Scheib, and F. Vogler, Phys. Lett. 88B, 51 (1979).

[14]J. Arvieux, J. P. Albanese, M. Buenerd, D. Lebrun, E. Boschitz, C. H. A. Ingram, and J. Jansen, Phys. Rev. Lett. 42, 753 (1979).

[15]P. D. Kunz, University of Colorado (private communication).

[16]G. R. Satchler, Part. Nucl. 5, 195 (1973); Nucl. Phys. A195, 1 (1972).

[17]T. J. Deal, Nucl. Phys. A217, 210 (1973); M. N. Harakeh, Phys. Lett. 90B, 13 (1980).

[18]D. H. Youngblood, A. D. Bacher, D. R. Brown, J. D. Bronson, J. M. Moss, and C. M. Rozsa, Phys. Rev. C 15, 246 (1977).

[19]K. T. Knöpfle, G. J. Wagner, H. Brener, M. Rogge, and C. Mayer-Boricke, Phys. Rev. Lett. 35, 779 (1975).

[20]M. N. Harakeh, A. R. Arends, M. J. A. De Voight, A. G. Drentje, S. Y. van der Werf, and A. van der Woude, Nucl. Phys. A265, 189 (1976).

[21]D. R. Brown, J. M. Moss, C. M. Rozsa, D. H. Youngblood, and J. D. Bronson, Nucl. Phys. A313, 157 (1979).